

# Detection of Conformational Changes along the Kinetic Pathway of Protein Kinase A Using a Catalytic Trapping Technique<sup>†</sup>

Jennifer Shaffer and Joseph A. Adams\*

Department of Pharmacology, University of California, San Diego, La Jolla, California 92093-0506

Received May 14, 1999; Revised Manuscript Received July 19, 1999

**ABSTRACT:** The dissociation rate constants for the two products of the reaction catalyzed by protein kinase A, ADP and phosphopeptide, were measured using a catalytic trapping technique to determine the role of product release in enzyme turnover. The enzyme was preequilibrated with ADP, and the reaction was initiated with a peptide substrate, LRRASLG, and ATP in a rapid quench flow instrument. At high, free magnesium concentrations (>2 mM), the large 'burst' in phosphopeptide production disappears, and, at low concentrations of free magnesium (0.5–1 mM), the kinetic transients become sigmoidal prior to the linear turnover phase. Increasing the concentrations of ATP or ADP did not influence the shape of the kinetic transients in the first 20 ms. ADP preequilibration protects the enzyme from inhibition by the covalent inactivator *p*-fluorosulfonylbenzoyl 5'-adenosine at 0.5 mM free magnesium, indicating that a competent E•ADP complex forms at low metal concentrations and the sigmoidal behavior in the catalytic trapping experiment is not due to free enzyme at high ATP concentrations. Simulations of the data indicate that ADP release is rate-limiting for turnover at high magnesium concentrations, but, at lower physiological levels of 0.5 and 1 mM, the off rate of ADP is 3- and 2-fold higher than  $k_{\text{cat}}$ , respectively. In contrast, the initial portions of the kinetic transients at 0.5 mM free magnesium were unaffected by phosphopeptide preequilibration, indicating that the release rate of this product is significantly larger than turnover. The transient kinetic data, coupled with a previous report [Shaffer and Adams (1999) *Biochemistry* 38, 5572–5581], support a phosphorylation mechanism under physiological magnesium concentrations that incorporates two partially rate-determining conformational changes, one prior to and one after the phosphoryl transfer step. We propose that the initial step activates the enzyme through key positioning of one or more active-site residues and the second step relaxes this conformation, a prerequisite for a subsequent catalytic cycle.

The catalytic subunit (C-subunit)<sup>1</sup> of protein kinase A (PKA) is liberated from its regulatory subunit by the binding of cAMP. The free C-subunit is active, catalyzes the phosphorylation of numerous protein targets on serine and threonine, and has widespread influence on many cellular processes ranging from carbohydrate metabolism to neurotransmitter biosynthesis [see review (1)]. Over the years PKA has become a paradigm for the enzyme family of protein kinases based on several attributes. First, active PKA can be obtained readily in large amounts either from tissue sources or in recombinant form (2). Second, the C-subunit of PKA (40 000 kDa) contains no covalently bound regulatory domains that influence activity. Third, PKA was the first protein kinase structure to be solved by X-ray diffraction methods. In recent years, PKA has been cocrystallized with various nucleotides, divalent metal ions, and inhibitor, substrate, and product peptides (3–6).

PKA will not phosphorylate proteins without the assistance of an essential, high-affinity  $\text{Mg}^{2+}$ . Based on X-ray data, this metal chelates the  $\beta$ - and  $\gamma$ -phosphates of ATP and is held in position by a conserved aspartic acid residue, Asp-184 (4). While this metal ion is sufficient for catalysis, a second, lower affinity site becomes occupied when the concentration of  $\text{Mg}^{2+}$  exceeds that for ATP, a condition found in living cells (7). This secondary metal chelates the  $\alpha$ - and  $\gamma$ -phosphates of ATP and is positioned by Asn-171 of the catalytic loop (4). This site has been termed the "inhibitory" site since its full occupancy reduces turnover ( $k_{\text{cat}}$ ) by 5–6-fold (8) but, under physiological concentrations of 0.5 mM free magnesium, the site will be occupied partially (approximately 20%) owing to an apparent dissociation constant of approximately 2 mM for the metal (8). Given these observations, a thorough understanding of the role of this secondary metal is critical for understanding the mechanism of phosphoryl transfer catalyzed by this essential protein kinase.

Although PKA has been studied extensively by steady-state kinetic techniques, the most detailed mechanistic information has been garnered from the application of pre-steady-state kinetic approaches. The phosphorylation of small peptides displays 'burst' kinetics under high magnesium concentrations (9, 10), a phenomenon that is consistent with

<sup>†</sup> This work was supported by NIH Grant GM 54846.

\* To whom correspondence should be addressed. Telephone: (858) 822-3360. Fax: (858) 822-3361. E-mail: joeadams@ucsd.edu.

<sup>1</sup> Abbreviations: C-subunit, catalytic subunit of protein kinase A; FSBA, *p*-fluorosulfonylbenzoyl 5'-adenosine; Kempptide, peptide sequence LRRASLG; Mops, 3-(*N*-morpholino)propanesulfonic acid; phosphokempptide, Kempptide phosphorylated on serine [LRRAS(P)LG]; PKA, cAMP-dependent protein kinase.

rapid phosphoryl transfer in the active site (approximately  $500\text{ s}^{-1}$ ). The linear portion of the phosphorylation reaction which corresponds to the steady-state kinetic rate is controlled by slow release of the product, ADP (11). While these studies were performed when most of the inhibitory site is occupied, recent experiments demonstrate that phosphoryl transfer is also fast at 0.5 mM free magnesium, conditions closely approximating the level of activating metal in the cell (12). These studies suggest that the second metal ion does not participate in the phosphoryl transfer step, an unusual finding given its direct interaction with the  $\gamma$ -phosphate of ATP. Nonetheless, these results do not provide any information on the nature of the rate-determining step in the reaction under low metal ion concentrations. To determine the rates of dissociation of the products, ADP and phosphopeptide, under different metal occupancy levels, a catalytic trapping procedure was employed. The data show that phosphopeptide release is fast at all levels of magnesium and ADP release and a conformational change are partially rate-limiting under physiological metal ion concentrations. The results demonstrate that conformational changes and ADP dissociation play equivalent roles in limiting turnover. In a previous study, we demonstrated that a conformational change precedes phosphoryl transfer and partially limits enzyme turnover at 0.5 mM free  $\text{Mg}^{2+}$  (12). These data support a coupled mechanism in which one conformational change precedes the phosphoryl transfer step and a second follows this step.

## MATERIALS AND METHODS

**Materials.** Adenosine triphosphate (ATP), *p*-fluorosulfonylbenzoyl 5'-adenosine (FSBA), 3-(*N*-morpholino)propanesulfonic acid (Mops), lactate dehydrogenase, pyruvate kinase, nicotinamide adenine dinucleotide, reduced (NADH), and phosphoenolpyruvate were purchased from Sigma Chemicals. Magnesium chloride, phosphoric acid, and liquid scintillant were obtained from Fisher Scientific. Phosphocellulose filter disks were purchased from Whatman, and [ $\gamma$ - $^{32}\text{P}$ ]ATP was obtained from NEN Products.

**Peptide and Enzyme.** The substrate peptide, LRRASLG (Kemptide), was synthesized at the USC Microchemical Core Facility using Fmoc chemistry and purified by C-18 reverse phase HPLC. The phosphorylated form of the substrate peptide [phosphokemptide; LRRAS(P)LG] was provided to us by Drs. Susan Taylor and John Lew. Kemptide concentrations were determined by turnover with the C-subunit under conditions of limiting peptide in the spectrophotometric assay. The purity of phosphokemptide was also determined by C-subunit turnover. Less than 1% of the total phosphokemptide contains Kemptide. Recombinant C-subunit was expressed in *E. coli* and purified according to previously published procedures (13). The concentration of the enzyme was measured by its absorbance at 280 nm ( $A_{0.1\%} = 1.2$ ).

**Coupled Enzyme Assay.** The enzymatic activity of the C-subunit was determined as described previously (8). The oxidation of NADH, monitored spectrophotometrically as an absorbance decrease at 340 nm, is coupled to the production of ADP by lactate dehydrogenase and pyruvate kinase. All reactions were measured in a Beckman DU640 spectrophotometer equipped with a microcuvette holder. Typical steady-state kinetic assays were performed in 50 mM Mops (pH 7)

in a final volume of 60  $\mu\text{L}$  at 24 °C. PKA (6–60 nM) was typically incubated with 0.005–2 mM ATP, varying free magnesium (0.5–10 mM), 1 mM phosphoenolpyruvate, 0.2 mM NADH, 12 units of lactate dehydrogenase, and 4 units of pyruvate kinase for several minutes before initiating the reaction with peptide. Background reactions were recorded in the absence of Kemptide but were never more than 3% of the Kemptide-dependent reaction over all substrate concentrations. The total concentration of  $\text{MgCl}_2$  needed to obtain a desired free concentration of  $\text{Mg}^{2+}$  was calculated based on the dissociation constants of 0.0143 mM for Mg-ATP, 5 mM for Mg-PEP, and 19.5 mM for Mg-NADH (14).

**Rapid Quench Flow Measurements.** Pre-steady-state kinetic measurements were made using a KinTek Corp. Quench Flow Apparatus, Model RGF-3, and a previously published procedure (9). Quench flow experiments were typically executed by loading equal volumes of enzyme, buffer, and magnesium chloride into one sample loop and Kemptide, [ $\gamma$ - $^{32}\text{P}$ ]ATP (600–2000 cpm pmol $^{-1}$ ), and magnesium chloride into the other in 50 mM Mops (pH 7) at 24 °C. For reactions performed in the presence of ADP or phosphokemptide, either product was included in the sample loop containing the enzyme. For experiments with preequilibrated ADP, a stability constant of 0.25 mM for Mg-ADP was used to obtain the correct free magnesium concentration (14). Unless otherwise designated in the text, the concentrations of the reactants represent those in the mixing chamber. The reactions were quenched using 30% acetic acid, and phosphokemptide was separated from unreacted ATP by a filter binding assay (15). A portion of each quenched reaction (55  $\mu\text{L}$ ) was spotted onto a phosphocellulose filter disk, washed 4 times with 0.5% phosphoric acid, rinsed with acetone, dried, and counted on the  $^{32}\text{P}$  channel in liquid scintillant. Control experiments were performed to determine the background phosphorylation (i.e., phosphorylation of peptide in the presence of quench) using previously published protocols (9). The specific activity of [ $\gamma$ - $^{32}\text{P}$ ]ATP was determined by measuring complete turnover of known, limiting amounts of Kemptide in the rapid quench flow instrument. The time-dependent concentration of phosphokemptide was then determined by considering the total counts per minute (CPM) on each disk, the specific activity of the labeled phosphopeptide, the total collected volume, and the background phosphorylation on washed filter disks as previously described (9).

**FSBA Inactivation.** FSBA (0.03–0.5 mM) was incubated with the C-subunit (10  $\mu\text{M}$ ) either in the absence or in the presence of varying ADP (0.5–4 mM) in 50 mM Mops (pH 7) containing 0.5 mM free magnesium (when ADP is present) and 1 mg/mL BSA in a total volume of 100  $\mu\text{L}$  at 30 °C. After designated time periods (0–60 min), small aliquots (5  $\mu\text{L}$ ) were removed and diluted 100-fold in cold Mops buffer (4 °C) to stop the reaction. A portion of this quenched reaction mix was then assayed immediately for kinase activity using the  $^{32}\text{P}$  assay and 10 mM free  $\text{Mg}^{2+}$ . Typically, 100  $\mu\text{L}$  of the quenched reaction was added to a 100  $\mu\text{L}$  mixture containing 2 mM ATP (approximately 200 CPM/pmol), 12 mM  $\text{MgCl}_2$ , and 400  $\mu\text{M}$  Kemptide in 100 mM Mops (pH 7). After varying time intervals, small volumes of this reaction (30  $\mu\text{L}$ ) were removed and added to 30  $\mu\text{L}$  of 30% acetic acid, and the phosphopeptide was measured as described in the previous section. Control experiments

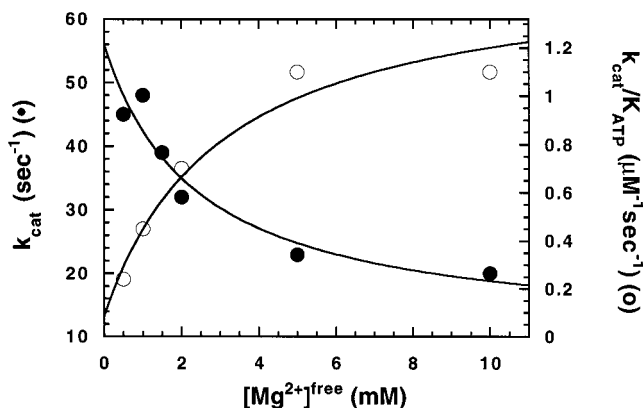


FIGURE 1: Steady-state kinetic parameters for the phosphorylation of Kemptide by PKA as a function of free  $Mg^{2+}$  concentration. C-subunit (20 nM) was preequilibrated with varying concentrations of ATP (5–2000  $\mu M$ ) at varied, fixed free  $Mg^{2+}$  concentrations (0.5–10 mM), and the reaction was initiated with 200  $\mu M$  Kemptide. The kinetic parameters,  $k_{cat}$  and  $k_{cat}/K_{ATP}$ , were determined from plots of initial velocity, measured in the coupled enzyme assay, versus ATP concentration. The turnover data were fit to a hyperbolic function to obtain  $k_{cat}$  values extrapolated to zero and infinite free  $Mg^{2+}$  concentrations of  $56 \pm 5$  and  $10 \pm 4$   $s^{-1}$  and an apparent metal affinity constant of  $2.4 \pm 0.9$  mM. The data were also fit to a hyperbolic function to obtain  $k_{cat}/K_{ATP}$  values extrapolated to zero and infinite free  $Mg^{2+}$  concentrations of  $0.09 \pm 0.04$  and  $1.5 \pm 0.51$   $\mu M^{-1} s^{-1}$  and an apparent metal affinity constant of  $3.1 \pm 1.3$  mM.

were performed in which no FSBA was added but no significant decrease in enzyme activity was measured after an incubation period of 60 min at 30 °C (data not shown). The FSBA stock (175 mM) was prepared in neat DMSO, but the final percent concentration of the solvent additive was less than 1% in the inactivation reaction mix.

## RESULTS

**Magnesium-Dependent Steady-State Kinetic Parameters for PKA.** The steady-state kinetic parameters for the C-subunit of PKA were measured as a function of free  $Mg^{2+}$  concentration using the coupled enzyme assay. C-subunit was preequilibrated with varying ATP concentrations and varied, fixed concentrations of free  $Mg^{2+}$  for approximately 3 min before initiating the reaction with Kemptide (200  $\mu M$ ). Plots of initial velocity versus ATP concentration provided the true  $K_m$  for ATP ( $K_{ATP}$ ) and  $k_{cat}$  since the concentration of Kemptide in all experiments was 20-fold higher than  $K_{peptide}$ , the  $K_m$  for peptide (8, 12). Plots of  $k_{cat}$  and  $k_{cat}/K_{ATP}$  are shown in Figure 1 as a function of free  $Mg^{2+}$  concentration. The data were fit to hyperbolic functions to determine the values of  $k_{cat}$  and  $k_{cat}/K_{ATP}$  at zero and infinite free  $Mg^{2+}$  concentrations and the apparent affinity constant of the metal (see legend of Figure 1). Occupancy of the second metal site reduces  $k_{cat}$  by 6-fold (56 versus 10  $s^{-1}$ ) and increases  $k_{cat}/K_{ATP}$  by 17-fold (0.09 versus 1.5  $\mu M^{-1} s^{-1}$ ). The apparent dissociation constant for the second metal is 2–3 mM.

**Inhibition of PKA by ADP and Phosphokemptide.** The inhibition constant for ADP ( $K_i$ ) was measured at 0.5 and 10 mM free  $Mg^{2+}$  using the  $^{32}P$  assay. It was shown previously that ADP is a competitive inhibitor with respect to ATP (8) so that Dixon plot analysis could be used to determine the true  $K_i$  from the apparent  $K_i$  value. Initial velocities were measured as a function of ADP using 500  $\mu M$  ATP and 200  $\mu M$  Kemptide.  $K_{ATP}$  values of 200  $\mu M$  at

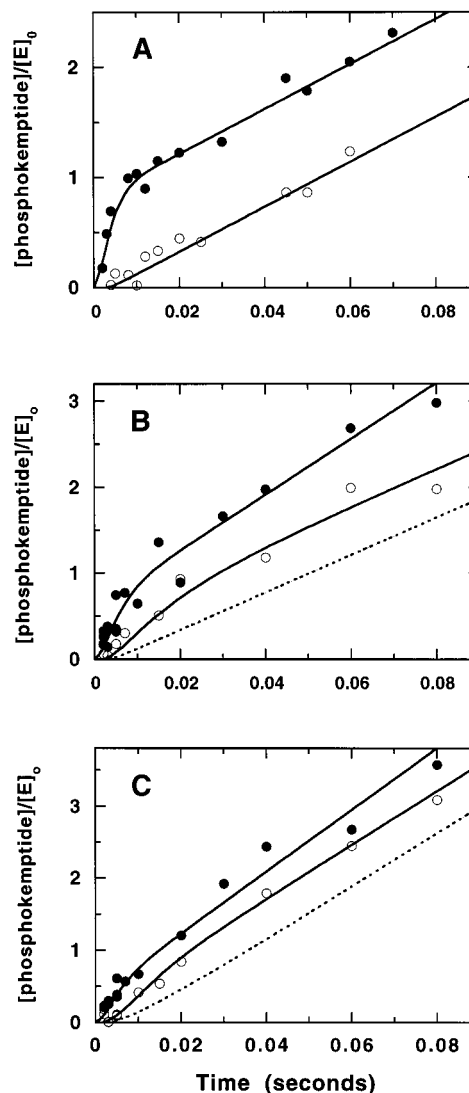


FIGURE 2: Time-dependent production of phosphokemptide in the absence (●) and presence (○) of ADP at 10 (A), 1 (B), and 0.5 (C) mM free  $Mg^{2+}$ . C-subunit (1.9, 2.1, and 3.5  $\mu M$  at 10, 1, and 0.5 mM free  $Mg^{2+}$ , respectively, in the mixing chamber) either alone or preequilibrated with 0.4 mM ADP (concentration prior to mixing) was mixed with 2 mM ATP and 200  $\mu M$  Kemptide in the rapid quench flow instrument. The designated free concentrations of metal were maintained in the sample loop containing the enzyme and the mixing chamber. The production of phosphokemptide is normalized to the enzyme concentration, and the lines drawn through the data were obtained from kinetic simulations (see text). The data in the absence of ADP were also fit analytically to obtain 'burst' rates, amplitudes, and linear rates of  $250 \pm 80$ ,  $0.93 \pm 0.09$ , and  $20 \pm 2$   $s^{-1}$  at 10 mM free  $Mg^{2+}$ ;  $250 \pm 60$ ,  $0.84 \pm 0.29$ , and  $31 \pm 5$   $s^{-1}$  at 1 mM free  $Mg^{2+}$ ; and  $150 \pm 50$ ,  $0.54 \pm 0.14$ , and  $49 \pm 6$   $s^{-1}$  at 0.5 mM free  $Mg^{2+}$ , respectively (fits not shown).

0.5 mM free  $Mg^{2+}$  and 10  $\mu M$  at 10 mM free  $Mg^{2+}$  (Figure 1) were used to measure true  $K_i$  values of  $37 \pm 11$  and  $10 \pm 3$   $\mu M$  at 0.5 and 10 mM free  $Mg^{2+}$ , respectively. Double reciprocal plots of  $v$  versus Kemptide concentration at 0, 1, 3, and 4 mM phosphokemptide and 2 mM ATP intersect at the  $1/v$  axis, indicating that phosphokemptide is a competitive inhibitor with respect to Kemptide (data not shown). The  $V_{max}$  values for these plots are  $58 \pm 8$ ,  $61 \pm 10$ ,  $58 \pm 13$ , and  $64 \pm 20$   $\mu M/min$  at 0, 1, 3, and 4 mM phosphokemptide, respectively. A plot of the slope of the Dixon plot versus  $1/[Kemptide]$  indicates that the true  $K_i$  for phosphokemptide at 0.5 mM free  $Mg^{2+}$  is  $360 \pm 60$   $\mu M$ . By comparison, ADP



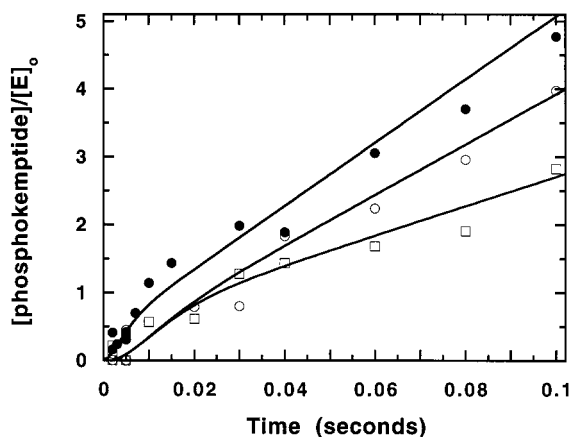


FIGURE 3: Time-dependent production of phosphokemptide in the absence (●) and presence (○, □) of varying ADP concentrations at 0.5 mM free  $Mg^{2+}$ . C-subunit (1.2  $\mu M$ ) either alone or preequilibrated with 0.4 (○) or 1 (□) mM ADP (concentration prior to mixing) was mixed with 2 mM ATP and 200  $\mu M$  Kemptide in the rapid quench flow instrument. The free concentration of metal was maintained in the sample loop containing the enzyme and the mixing chamber. The production of phosphokemptide was normalized to the enzyme concentration, and the lines drawn through the data were obtained from kinetic simulations (see text).

binds approximately 10-fold more tightly than phosphokemptide to the C-subunit at 0.5 mM free  $Mg^{2+}$ .

**Catalytic Trapping Experiments: ADP Preequilibration.** A catalytic trapping protocol was used to determine the dissociation rate constant for ADP as a function of free  $Mg^{2+}$  concentration. In this experiment, C-subunit and ADP were preequilibrated, and the reaction was initiated with Kemptide and ATP under conditions of varied, fixed free magnesium. Typical kinetic transients for these experiments are shown in Figure 2 at 0.5, 1, and 10 mM  $Mg^{2+}$ . In each study, the C-subunit is preequilibrated with 0.4 mM ADP (concentration prior to mixing), an amount that is, at least, 10-fold higher than the nucleotide's  $K_i$  value over the entire concentration range of free metal. Control experiments were performed under identical conditions except ADP was omitted from the reaction. In each case, the enzyme or enzyme-ADP complex was mixed with 2 mM ATP and 200  $\mu M$  Kemptide. These kinetic studies were also performed at 2, 4, and 5 mM free  $Mg^{2+}$  under identical concentrations of ATP, ADP, and Kemptide (data not shown). At 0.5, 1, and 10 mM free  $Mg^{2+}$ , increasing the concentration of ATP to 3 mM did not have any significant effects on the kinetic transients, indicating that this concentration range is sufficient to trap the enzyme once ADP dissociates (data not shown). To ensure that all the free enzyme at low metal concentrations is complexed with ADP, trapping studies were performed at higher concentrations of ADP. A plot of phosphokemptide production versus time at 0, 0.4, and 1 mM ADP (concentration prior to mixing) and 0.5 mM free  $Mg^{2+}$  is shown in Figure 3. Increasing the concentration of ADP did not affect the first 20 ms of the transient although the slope of the linear portion of the reaction was reduced. The lines drawn through the data in Figures 2 and 3 were generated from kinetic modeling using numerical integration (see Discussion).

**FSBA Inactivation Experiments.** It was shown previously that FSBA inactivates the C-subunit of PKA in a time-dependent manner by covalently modifying the active-site

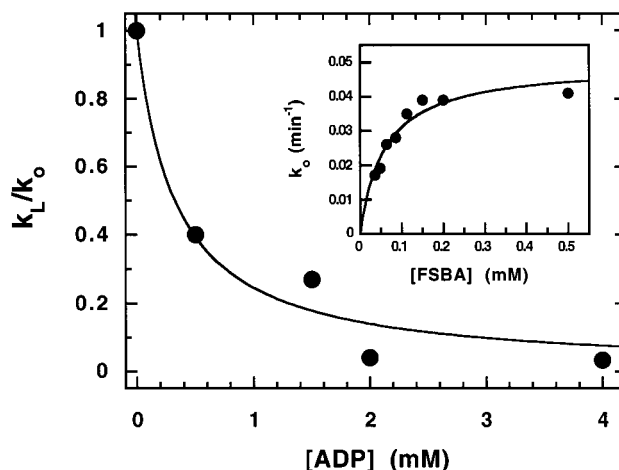


FIGURE 4: Inactivation of the C-subunit by FSBA in the absence and presence of varying concentrations of ADP at 0.5 mM free  $Mg^{2+}$ . The rate of inactivation was measured from the time-dependent decrease in enzyme activity using 0.2 mM FSBA and is expressed as a ratio of the inactivation rates in the presence ( $k_L$ ) and absence ( $k_0$ ) of varying ADP concentrations. The effects of FSBA concentration on the inactivation rate in the absence of ADP are shown in the inset. The data fitting is described in the text.

residue Lys-72 (16, 17). Protection from inactivation can be achieved by preincubation with ATP or ADP under conditions of 8 or 9 mM free  $Mg^{2+}$ , confirming that FSBA is directed at the ATP binding site and that both nucleotides can form a stable complex with the enzyme under these metal ion concentrations. FSBA inactivation experiments were performed with PKA to determine whether ADP can protect the enzyme under physiological concentrations of free magnesium (0.5 mM). The rates of FSBA inactivation were measured in the absence ( $k_0$ ) and presence ( $k_L$ ) of varying ADP concentrations by monitoring the initial velocity of the enzyme reaction as a function of FSBA incubation time. As shown in Figure 4, increasing the concentration of ADP in the FSBA reaction significantly reduces the rate of inactivation and protects the enzyme from inactivation.

The inactivation data in Figure 4 were fit to eq 1 which is a nonlinearized form of a previously published kinetic treatment for irreversible inactivation in the presence of a competing ligand (18).

$$k_L/k_0 = \frac{A}{[L] + A} \quad (1)$$

where

$$A = \frac{K_d\{K_i + [I]\}}{K_i}$$

In eq 1,  $K_i$  and  $K_d$  are the dissociation constants for FSBA and ADP and  $[I]$  and  $[L]$  are the concentrations of FSBA and ADP in the inactivation reaction. The  $K_i$  for FSBA was measured by monitoring the time-dependent inactivation of PKA at a series of FSBA concentrations (inset of Figure 4). The hyperbolic response is consistent with the reversible formation of an enzyme-inhibitor complex prior to covalent modification. The values of  $K_i$  and  $k_2$  (the maximum rate of inactivation) are  $60 \pm 8 \mu M$  and  $0.05 \pm 0.003 \text{ min}^{-1}$ , respectively. A fit of the data in Figure 4 to eq 1 using the  $K_i$  provides a  $K_d$  for ADP of  $70 \pm 16 \mu M$ , a value that is

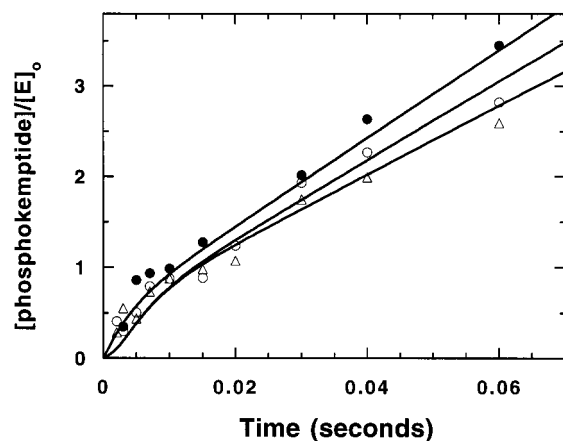


FIGURE 5: Time-dependent production of phosphokemptide in the absence (●) and presence of varying concentrations of unlabeled phosphokemptide (○, △) at 0.5 mM free  $Mg^{2+}$ . C-subunit (4.2  $\mu M$ ) either alone or preequilibrated with 4 (○) or 6 (△) mM phosphokemptide (concentration prior to mixing) was mixed with 2 mM ATP and 200  $\mu M$  Kemptide in the rapid quench flow instrument. The free concentration of metal was maintained in the sample loop containing the enzyme and the mixing chamber. The production of phosphokemptide is normalized to the enzyme concentration, and the lines drawn through the data were obtained from kinetic simulations (see text). The data in the absence of phosphokemptide were also fit analytically to obtain a 'burst' rate, amplitude, and linear rate of  $200 \pm 50 s^{-1}$ ,  $0.60 \pm 0.14$ , and  $48 \pm 6 s^{-1}$  (fits not shown).

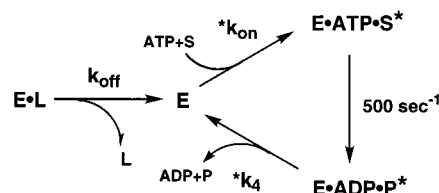
less than 2-fold larger than the  $K_I$  for ADP (37  $\mu M$ ) measured from product inhibition studies.

**Catalytic Trapping Experiments: Phosphokemptide Preequilibration.** A catalytic trapping protocol was used to determine the dissociation rate constant for phosphokemptide. In this experiment, C-subunit and unlabeled phosphokemptide were preequilibrated, and the reaction was initiated with Kemptide and ATP under conditions of 0.5 mM free  $Mg^{2+}$ . Control experiments were performed under identical conditions except phosphokemptide was omitted from the reaction. Typical kinetic transients for these experiments are shown in Figure 5. In each study, the C-subunit is preequilibrated with 4 and 6 mM phosphokemptide (concentration prior to mixing), an amount that is 10- and 17-fold higher than the product's  $K_I$  value. Phosphokemptide did not have a significant effect on the first 10 ms of the reaction although the slope of the linear portion of the transients ( $>20$  ms) decreased at higher phosphokemptide concentrations. The lines drawn through the data in Figure 5 were generated from kinetic modeling using numerical integration (see Discussion).

## DISCUSSION

**Magnesium Dependence on the Steady-State Kinetic Parameters.** Although PKA can bind two magnesium ions in the active site, an essential, tight binding metal and a nonessential, low-affinity metal, the second magnesium ion has intermediate to low occupancy under physiological concentrations. In addition, the second metal ion profoundly influences the steady-state kinetic parameters for the enzyme (8, 12, 19). Figure 1 shows the effects of varying free magnesium concentrations on two kinetic parameters ( $k_{cat}$  and  $k_{cat}/K_{ATP}$ ) for the recombinant mouse C-subunit. While  $k_{cat}/K_{ATP}$  increases by 17-fold,  $k_{cat}$  decreases by 6-fold upon

Scheme 1



binding of the second metal. Both isotope partitioning and viscosometric studies suggest that the former increase is due to an enhanced encounter rate between ATP and the enzyme in the presence of the second metal ion (12, 19). By comparison, it has been suggested that the decrease in  $k_{cat}$  may be due to tighter binding of one of the products, ADP, at high free  $Mg^{2+}$  concentrations (19). Indeed, the  $K_I$  for ADP in the bovine C-subunit decreases as the free concentration of metal activator increases (8). Likewise, for the recombinant mouse C-subunit, the  $K_I$  for ADP decreases from 37 to 10  $\mu M$  and  $k_{cat}$  decreases 2.2-fold as the free concentration of  $Mg^{2+}$  is increased from 0.5 to 10 mM (Figure 1). These observations suggest that ADP release may completely limit turnover over all concentrations of magnesium.

**Influence of ADP on the Pre-Steady-State Kinetics at 10 mM Free  $Mg^{2+}$ .** The phosphorylation of small peptide substrates by PKA has been studied using fast mixing techniques at both physiological and nonphysiological concentrations of  $Mg^{2+}$ . At 10 and 0.5 mM free  $Mg^{2+}$ , the reaction is biphasic with a rapid, stoichiometric 'burst' in phosphokemptide production followed by a slower linear phase when the enzyme is preequilibrated with ATP. These data indicate that Kemptide is phosphorylated rapidly in the active site at a rate of approximately  $500 s^{-1}$  (9, 12), a rate constant that exceeds turnover by more than 10-fold. To determine whether alterations in the ADP dissociation rate constant can explain the increase in  $k_{cat}$  at lower magnesium concentrations, a catalytic trapping experiment was applied. In this experiment, C-subunit and ADP are preequilibrated and rapidly mixed with Kemptide and ATP, and the production of phosphokemptide is monitored. The results of this experiment at 10 mM free  $Mg^{2+}$  are shown in Figure 2A. The large, stoichiometric 'burst' in phosphokemptide production disappears and is replaced by a small lag phase upon ADP preequilibration. This has been observed previously for PKA under identical metal ion concentrations and is consistent with a kinetic mechanism in which ADP release controls turnover (11).

The data in Figure 2A were fit to the kinetic mechanism shown in Scheme 1 using the numerical integration program KINSIM (20) where L is ADP,  $k_{off}$  is the dissociation rate constant for L,  $*k_{on}$  is the observed net association rate constant for both Kemptide (S) and ATP, and  $*k_4$  is the observed net dissociation rate constant for the products. Both  $*k_{on}$  and  $*k_4$  are composite rate constants that may include conformational changes, binding steps, and the formation of mixed complexes. In the last case, the formation of a mixed complex implies that free enzyme does not form so that E, as written in Scheme 1, could represent another steady-state species such as E·S if phosphokemptide release is fast and E·ADP·S can form or E·ATP if ADP release is fast and E·ATP·P can form. In either scenario, the order of addition

Table 1: Simulation Parameters for Kemptide Phosphorylation in the Absence and Presence of ADP at 0.5, 1, and 10 mM Free  $\text{Mg}^{2+}$ <sup>a</sup>

[ $\text{Mg}^{2+}$ ] <sub>free</sub> (mM)	[ADP] (mM) <sup>b</sup>	* $k_{\text{on}}[\text{ATP}][\text{S}]$ ( $\text{s}^{-1}$ )	* $k_4$ ( $\text{s}^{-1}$ )	$k_{\text{off}}$ ( $\text{s}^{-1}$ )	$\nu^{\text{calc}}/[\text{E}]_0$ ( $\text{s}^{-1}$ ) <sup>c</sup>	$\nu^{\text{obs}}/[\text{E}]_0$ ( $\text{s}^{-1}$ ) <sup>d</sup>
0.5	none	180	70		45	44
0.5	0.4	180	53	140	37	30
0.5	1.0	180	25	130	21	19
1	none	350	45		37	39
1	0.4	350	27	80	24	31
10	none	400	23		21	20
10	0.4	400	21	23	19	18

<sup>a</sup> The simulated kinetic parameters were obtained by fitting the data in Figures 2 and 3 to the kinetic mechanism in Scheme 1. For all simulations, the rate of phosphoryl transfer is fixed at  $500 \text{ s}^{-1}$ . <sup>b</sup> These values are the concentrations of ADP preequilibrated with PKA prior to mixing. <sup>c</sup> These linear rate constants were determined from simulations using the data in the table. <sup>d</sup> These linear rate constants were determined from steady-state kinetic analyses using the  $^{32}\text{P}$  assay under identical conditions as those in the legends of Figures 2 and 3 except the enzyme concentrations were lower.

and release of the nucleotides and peptides would be different than depicted in Scheme 1 but would not affect the salient features of the kinetic simulations (vide infra). Initially, the kinetic transient in the absence of ADP (i.e., no L) was modeled adequately using the kinetic constants shown in Table 1 at 10 mM free  $\text{Mg}^{2+}$ . In the presence of ADP, the kinetic data can be interpreted according to Scheme 1 if the  $k_{\text{off}}$  for ADP is  $23 \text{ s}^{-1}$  and limits  $k_{\text{cat}}$  (Table 1). For the experiment in Figure 2A, the concentration of ADP, prior to mixing, is 40-fold larger than  $K_1$  so that all the free enzyme is presumably bound with this product. Increasing the concentration of ATP from 2 to 3 mM at  $200 \mu\text{M}$  Kemptide did not have any effect on the kinetic transients, indicating that all free enzyme resulting from ADP release is readily trapped (data not shown). We also treated the data in Figure 2A assuming that  $\text{E} \cdot \text{ADP} \cdot \text{S}$  can form, but this did not affect the simulations and the measurement of  $k_{\text{off}}$  since the values in Table 1 are net rate constants (data not shown).

**Influence of ADP on the Pre-Steady-State Kinetics at Varying Free  $\text{Mg}^{2+}$ .** The catalytic trapping studies presented in Figure 2A were repeated under varying concentrations of free, activating metal to determine the role of ADP release in turnover. Figure 2B,C presents the pre-steady-state kinetic transients for Kemptide phosphorylation at 1 and 0.5 mM free  $\text{Mg}^{2+}$  in the absence and presence of ADP preequilibration. In the absence of ADP, a large, stoichiometric ‘burst’ in phosphokemptide is observed at 1 mM free magnesium while a smaller, substoichiometric ‘burst’ is observed at 0.5 mM free magnesium. The latter result has been observed previously for PKA under this metal concentration and has been attributed to a slow conformational change step ( $180 \text{ s}^{-1}$ ) that precedes phosphoryl transfer (12). Since the concentrations of ATP and peptide substrate exceed both their  $K_m$  and  $K_d$  values, the reduced rate and amplitude cannot be attributed to low population of the central ternary complex. When the pre-steady-state kinetics were performed with enzyme preequilibrated with ATP at 0.5 mM free  $\text{Mg}^{2+}$ , a stoichiometric ‘burst’ amplitude and rate constant were observed (12). We simulated both kinetic transients in Figure 2B,C using the kinetic parameters in Table 1 and the kinetic mechanism in Scheme 1. The slow conformational change at 0.5 mM free magnesium is included in the ATP/S binding

step ( $*k_{\text{on}}[\text{ATP}][\text{S}]$ ) and results in a lower, observed binding rate (compare  $170 \text{ s}^{-1}$  at 0.5 mM and  $350 \text{ s}^{-1}$  at 1 mM free  $\text{Mg}^{2+}$ ). This slow conformational change does not appear at 1 mM free magnesium since a larger value was used for the ATP/S binding step and the apparent ‘burst’ amplitude is larger at 1 versus 0.5 mM metal.

The kinetic transients in Figure 2B,C in the presence of ADP (0.4 mM prior to mixing) were simulated using numerical integration, and the best fits to the data sets are shown in Table 1. The dissociation rate constants for ADP ( $k_{\text{off}}$ ) required to simulate the data sets were 2- and 3-fold higher than  $k_{\text{cat}}$  at 1 and 0.5 mM free  $\text{Mg}^{2+}$ , respectively (Table 1 and Figure 1). The values of  $k_{\text{off}}$  and  $k_{\text{cat}}$  are 140 and  $48 \text{ s}^{-1}$  at 0.5 mM and 80 and  $42 \text{ s}^{-1}$  at 1 mM free  $\text{Mg}^{2+}$ , respectively. The dotted lines in Figure 2B,C represent kinetic simulations when  $k_{\text{off}}$  is close to the value for  $k_{\text{cat}}$  but, in both cases, the simulations do not model accurately the experimental transients. These results support a model in which ADP release does not solely limit turnover at low magnesium concentrations. For simulations in the presence of ADP, good fitting to the linear portion of the data is obtained when lower values of  $*k_4$  are used compared to the control experiments in the absence of ADP. These adjustments in the parameter are consistent with the comparative levels of ATP and ADP used in the trapping experiments and represent small levels of product inhibition. At all concentrations of ADP, the rate of the linear portion of the reaction measured under steady-state kinetic assay conditions ( $\nu^{\text{obs}}/[\text{E}]_0$ ) is consistent with the simulated data values ( $\nu^{\text{calc}}/[\text{E}]_0$ ) (Table 1). Increasing the ADP concentration from 0.2 to 0.5 mM (concentrations in the mixing chamber) did not influence the first 20 ms of the reaction (Figure 3), the time at which ADP is expected to dissociate.

**Does a Stable  $\text{E} \cdot \text{ADP}$  Complex Form at 0.5 Free  $\text{Mg}^{2+}$ ?** The determination of a dissociation rate constant for ADP at low magnesium concentrations in the catalytic trapping experiments depends on the ability to form a stable, binary complex,  $\text{E} \cdot \text{ADP}$ , prior to the addition of ATP and Kemptide. The progressive shift in the catalytic trapping experiments to sigmoidal kinetics at 0.5 and 1 mM free  $\text{Mg}^{2+}$  (Figure 2) could be due to the inability to form this complex and a subsequent increase in the concentration of free enzyme prior to mixing rather than to an increased off rate for ADP. Indeed, there has been one report that the binding of ADP and phosphokemptide for the bovine enzyme is ordered in the reverse reaction (i.e., phosphorylation of ADP) at 0.5 mM free  $\text{Mg}^{2+}$  with phosphokemptide binding prior to ADP (21). In such a mechanism, ADP would dissociate before phosphokemptide in the forward reaction, a scenario opposite to the reaction sequence at 10 mM free  $\text{Mg}^{2+}$  (11). Although we measured a lower  $K_1$  for ADP compared to phosphokemptide (37 versus  $360 \mu\text{M}$ ) at 0.5 mM free  $\text{Mg}^{2+}$ , ADP may bind to and dissociate exclusively from a product ternary complex (e.g.,  $\text{E} \cdot \text{ADP} \cdot \text{P}$ ) and may have little or no affinity for the free enzyme. To determine whether ADP can bind PKA at low magnesium, FSBA inactivation experiments were conducted (Figure 4). Not only was ADP capable of protecting PKA from inactivation but also the concentration response of the inactivation curve indicates that ADP binds well to the free enzyme ( $K_d = 70 \mu\text{M}$ ). Using the FSBA-derived  $K_d$  for ADP, the enzyme is, at least, 85% saturated with ADP prior to mixing. These results indicate that the



sigmoidal behavior in the catalytic trapping experiments in Figures 2 and 3 is due to fast dissociation of ADP from either the  $E \cdot ADP$  or the  $E \cdot ADP \cdot S$  complexes.

**Does Phosphokemptide Release Affect Turnover?** At high free  $Mg^{2+}$  concentration, ADP release completely controls turnover, but at lower free  $Mg^{2+}$  concentration, ADP is only partially rate-limiting (Figure 2 and Table 1). Since phosphoryl transfer is fast over a wide range of magnesium concentrations (9, 12), we considered whether the release of phosphokemptide could play a role in controlling turnover. To address this question, the catalytic trapping experiment was adapted to measure the off rate of phosphokemptide. Preequilibration of the C-subunit with either 4 or 6 mM phosphokemptide (concentrations 11- or 17-fold above  $K_I$ ) had no significant effect on the 'burst' phase at 0.5 mM free  $Mg^{2+}$  (Figure 5). The data in Figure 5 were fit adequately to the kinetic mechanism in Scheme 1 (where L is now phosphokemptide) using values of 180 and 70  $s^{-1}$  for  $k_{on}[ATP][S]$  and  $k_4$  in the absence of phosphokemptide. Both transients in the presence of phosphokemptide were fit using a lower limit of 600  $s^{-1}$  for  $k_{off}$  and values of 60 and 50  $s^{-1}$  for  $k_4$  at 2 and 3 mM phosphokemptide, respectively. Since it is difficult to distinguish between the traces in the early reaction times, the off rate of phosphokemptide could be much higher than 600  $s^{-1}$ . Also, the small reduction in the linear phase rates in Figure 5 is consistent with the expected effects from product inhibition. The calculated values ( $v^{calc}/[E]$ ) for the steady-state rate are 45, 42, and 36  $s^{-1}$  at 0, 2, and 3 mM phosphokemptide, respectively, and compare well with the experimental values ( $v^{obs}/[E]$ ) of 43, 38, and 32  $s^{-1}$  at 0, 2, and 3 mM phosphokemptide, respectively.

While we have asserted that the data in Figure 5 imply that phosphokemptide release is fast, we have considered an alternative description as well. The absence of any effect of 4 and 6 mM phosphokemptide on the early portion of the kinetic transients could be due to large amounts of free enzyme prior to reaction initiation with ATP and substrate. For this scenario, we predict that the  $K_d$  for the product would need to be in excess of 20 mM to produce such a result. This enforces an ordered release of phosphokemptide followed by ADP since the  $K_I$  for the phosphopeptide is, at least, 100-fold lower than the  $K_d$  (compare  $K_I = 370 \mu M$  and  $K_d > 20$  mM). In this hypothetical mechanism, phosphokemptide could bind well in the presence of ADP ( $E \cdot ADP \cdot P$ ) and explain the low  $K_I$  versus  $K_d$ , but it is still difficult to account for partial rate limitation in the release of this product for several reasons: (1) The  $k_{cat}$  values for a series of peptide substrates are similar although the affinities of the inhibitor versions of these peptides (i.e., alanine substitution at serine) vary from 0.04 to 350  $\mu M$  (22, 23). (2) Kemptide dissociates from PKA at a rate in great excess of 500  $s^{-1}$  at all concentrations of free magnesium (12). Since phosphokemptide has lower affinity than Kemptide at 0.5 mM free  $Mg^{2+}$  (12), this product is likely to dissociate at a fast rate. (3) The rate-limiting step in turnover for the phosphorylation of the tight binding peptide substrate GRTGRRNSI is ADP release (11) even though the inhibitor form of this substrate (GRTGRRNAI) binds with a  $K_I$  of 40 nM (23). (4) The turnover number for GRTGRRNSI is 18 and 46  $s^{-1}$  at 10 and 0.5 mM free  $Mg^{2+}$ , respectively (24). These values are similar to those for Kemptide (Figure 1) although

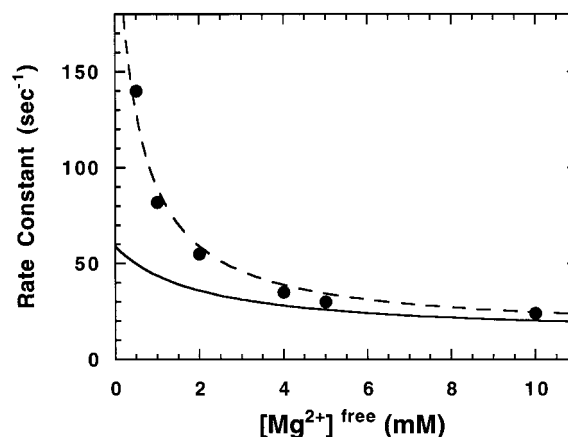


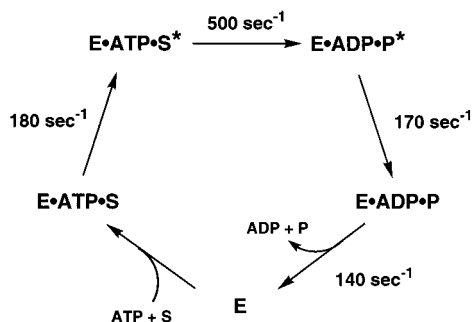
FIGURE 6: Effects of free  $Mg^{2+}$  on the dissociation rate constant for ADP. The data were determined from simulations of the pre-steady-state kinetic transients in the presence of ADP (see text). The dashed line is a hyperbolic fit to the data and indicates that the dissociation rate constant for ADP at zero and infinite free  $Mg^{2+}$  is approximately 240 and 14  $s^{-1}$  and the affinity constant for the metal is approximately 0.5 mM. The solid line represents the data fit for the dependence of  $k_{cat}$  on the free magnesium concentration (extracted from Figure 1).

GRTGRRNSI binds PKA about 1000-fold more tightly. These observations, coupled with the data in Figure 5, suggest that phosphokemptide dissociates rapidly at both 0.5 and 10 mM free  $Mg^{2+}$  and does not participate in the rate limitation of turnover.

**Conformational Changes in PKA.** Several biophysical studies have provided good evidence that conformational changes occur in the C-subunit of PKA upon ligand association. Based on small-angle X-ray scattering measurements, the radius of gyration of the enzyme decrease by 9% upon binding of the protein kinase inhibitor, PKI (25). This structural change in the protein was attributed to relative movements in the ATP and substrate binding domains and is supported by X-ray crystallographic analyses which show that the C-subunit may adopt either an "open" or a "closed" conformation (26). More recently, a protein footprinting technique was used to show that several critical loop segments exhibit altered reactivities in the presence of ATP, suggesting that they are involved in conformational changes upon nucleotide binding (27). In a previous report, we demonstrated that a conformational change (180  $s^{-1}$ ) precedes the phosphoryl transfer step in PKA at 0.5 mM free  $Mg^{2+}$  (12). This step is nucleotide-linked since it is observed only when the reaction is initiated with ATP and it disappears when ATP is pre-equilibrated with the enzyme prior to reaction initiation with Kemptide. Given these kinetic observations, this conformational change may have some structural ties to the equilibrium changes reported from footprinting experiments.

If we presume that the off rates of ADP from the pre-equilibrated  $E \cdot ADP$  binary complexes are the same as those from the enzyme under catalytic cycling, the experimental data presented herein suggest that a conformational change occurs after the phosphoryl transfer step and partially limits turnover at 0.5 and 1 mM free  $Mg^{2+}$ . Figure 6 shows a plot of the dissociation rate constant for ADP measured by the catalytic trapping experiments as a function of free metal concentration. The methodology employed in determining these values is identical to that used for the data

Scheme 2



fitting in Figures 2 and 3. Figure 6 shows that ADP release solely limits turnover at high free  $\text{Mg}^{2+}$  concentrations ( $>2$  mM) and only partially limits turnover at low, physiological levels. Since phosphokemptide release and phosphoryl transfer are fast at 0.5 mM free magnesium, a conformational change step which occurs after the catalytic step must provide the additional kinetic event that limits turnover. To account for the observed  $k_{\text{cat}}$  value at 0.5 mM free metal, this conformational change step must have a forward net rate constant of approximately  $170 \text{ s}^{-1}$ . Although it is not precisely clear when this step occurs with respect to the dissociation of ADP, we suggest that it is mechanistically distinct from the structural change that occurs prior to phosphoryl transfer. We base this supposition on review of the net rates of the reaction. If the conformational change observed prior to phosphoryl transfer is the only structural step in the pathway involved in rate limitation, the predicted  $k_{\text{cat}}$  for PKA at 0.5 mM free  $\text{Mg}^{2+}$  would be  $70 \text{ s}^{-1}$ , a value much higher than the true  $k_{\text{cat}}$  of  $45 \text{ s}^{-1}$  (Figure 1). Guided by this logic, a second, unique conformational change is essential for a satisfactory description of substrate phosphorylation.

Scheme 2 depicts a simple mechanism that describes the kinetic data collected at 0.5 mM free  $\text{Mg}^{2+}$ . In this scheme, we represent the first conformational change as occurring after ATP and substrate binding and prior to phosphoryl transfer but recognize that it may occur prior to ligand binding (12). The second conformational change step occurs after phosphoryl transfer, but its exact position with respect to ADP dissociation is not known. Although this mechanism is reported at low metal ion concentrations, it is likely that these conformational changes occur at high magnesium concentrations but are faster than our detection limits. At this point, it is difficult to know what structural changes are responsible for either conformational event but the observation that the first is ATP-linked (12) and the precedence stated above suggest that both may be associated with nucleotide binding. In such a mechanism, the first conformational change may orient ATP and several active-site residues for efficient catalysis and the second may relax this conformation, thereby permitting release of ADP and completion of the catalytic cycle. The similarity of the net rate constants for the two conformational changes (180 and  $170 \text{ s}^{-1}$ ) could be coincidental but may reflect the structural linkage and symmetry of the steps.

## ACKNOWLEDGMENT

We thank Dr. John Lew and Dr. Susan S. Taylor for providing us with the purified phosphokemptide,

LRRAS(P)LG.

## REFERENCES

- Barritt, G. J. (1992) in *Communication within animal cells*, pp 100–102, Oxford University Press, New York.
- Slice, L. W., and Taylor, S. S. (1989) *J. Biol. Chem.* 264, 20940–20946.
- Madhusudan, Trafny, E. A., Xuong, N., Adams, J. A., Ten Eyck, L. F., Taylor, S. S., and Sowadski, J. M. (1994) *Protein Sci.* 3, 176–187.
- Zheng, J., Knighton, D. R., Ten Eyck, L. F., Karlsson, R., Xuong, N., Taylor, S. S., and Sowadski, J. M. (1993) *Biochemistry* 32, 2154–2161.
- Zheng, J., Trafny, E. A., Knighton, D. R., Xuong, N., Taylor, S. S., Ten Eyck, L. F., and Sowadski, J. M. (1993) *Acta Crystallogr. D* 49, 362–365.
- Knighton, D. R., Zheng, J., Ten Eyck, L. F., Ashford, V. A., Xuong, N., Taylor, S. S., and Sowadski, J. M. (1991) *Science* 253, 407–414.
- Romani, A., and Scarpa, A. (1992) *Arch. Biochem. Biophys.* 298, 1–12.
- Cook, P. F., Neville, M. E., Vrana, K. E., Hartl, F. T., and Roskoski, J. R. (1982) *Biochemistry* 21, 5794–5799.
- Grant, B., and Adams, J. A. (1996) *Biochemistry* 35, 2022–2029.
- Zhou, J., and Adams, J. A. (1997) *Biochemistry* 36, 2977–2984.
- Zhou, J., and Adams, J. A. (1997) *Biochemistry* 36, 15733–15738.
- Shaffer, J., and Adams, J. A. (1999) *Biochemistry* 38, 5572–5581.
- Yonemoto, W., McGlone, M. L., Slice, L. W., and Taylor, S. S. (1991) in *Protein Phosphorylation (Part A)* (Hunter, T., and Sefton, B. M., Eds.) pp 581–596, Academic Press, Inc., San Diego.
- Martell, A. E., and Smith, R. M. (1977) *Critical Stability Constants*, Vol. 3, Plenum, New York.
- Kemp, B. E., Graves, D. J., Benjamini, E., and Krebs, E. G. (1977) *J. Biol. Chem.* 252, 4888–4894.
- Hixson, C. S., and Krebs, E. G. (1979) *J. Biol. Chem.* 254, 7509–7514.
- Zoller, M. J., and Taylor, S. S. (1979) *J. Biol. Chem.* 254, 8363–8367.
- Carillo, N., Arana, J. L., and Vallejos, R. H. (1981) *J. Biol. Chem.* 256, 6823–6828.
- Kong, C.-T., and Cook, P. F. (1988) *Biochemistry* 27, 4795–4799.
- Barshop, B. A., Wrenn, R. F., and Frieden, C. (1983) *Anal. Biochem.* 130, 134–145.
- Qamar, R., Yoon, M.-Y., and Cook, P. F. (1992) *Biochemistry* 31, 9986–9992.
- Mitchell, R. D., Glass, D. B., Wong, C., Angelos, K. L., and Walsh, D. A. (1995) *Biochemistry* 34, 528–534.
- Glass, D. B., Cheng, H.-C., Mende-Mueller, L., Reed, J., and Walsh, D. A. (1989) *J. Biol. Chem.* 264, 8802–8810.
- Ne, D. Q. (1999) personal communication.
- Olah, G. A., Mitchell, R. D., Sosnick, T. R., Walsh, D. A., and Trehwella, J. (1993) *Biochemistry* 32, 3649–3657.
- Zheng, J., Knighton, D. R., Xuong, N., Taylor, S. S., Sowadski, J. M., and Ten Eyck, L. F. (1993) *Protein Sci.* 2, 1559–1573.
- Cheng, X., Shaltiel, S., and Taylor, S. S. (1998) *Biochemistry* 37, 14005–14013.

BI991109Q